Research on Filtering Method of Increment Capacity Analysis Curve of Ternary Lithium Ion Battery

IOP Conf. Series: Materials Science and Engineering **486** (2019) 012075 doi:10.1088/1757-899X/486/1/012075

Research on Filtering Method of Increment Capacity Analysis Curve of Ternary Lithium Ion Battery

Zhang Qi[1], Wu Jian[1], Wang Zhanguo[1], Zhang Yanru[1] and Mu Biqiang[2]

[1] National Active Distribution Network Technology Research Center (NANTEC) (Beijing Jiaotong University), Haidian District, Beijing 100044, China
[2] Academy of Mathematics and Systems Science, Chinese Academy of Sciences, Haidian District, Beijing 100044, China

jianwu@bjtu.edu.cn

Abstract. Increment Capacity Analysis method has been widely concerned by experts and scholars because it can analyze the battery chemical reaction without destroying the physical structure of the battery. However the inevitable noise on the capacity increment curve brings huge damage to the analysis of the battery reaction process. In this paper, the influence of different voltage intervals on the ICA curve is analyzed firstly, then a certain voltage interval is selected, and the capacity increment curve is filtered by Gaussian process regression and wavelet transform. Compared with the original unfiltered ICA curve, the proposed method is verified feasible.

1. Introduction

As an in-situ non-destructive electrochemical analysis method, Incremental Capacity Analysis (ICA) can study the electrochemical reaction inside the battery without destroying the physical structure of the battery. Many scholars use it to analyse different performance indicators such as SOC, SOH, and remaining available capacity of the battery [1]-[4]. Lithium-ion battery has a distinct platform stage on its charging curve (the horizontal axis is the capacity and the vertical axis is the voltage), which is reflected in the internal battery, during the chemical reaction period, the battery's charge is greatly increased, and the corresponding voltage does not rise obviously. So the conclusion that the chemical reaction inside the battery is the most intense during this period can be obtained. This is also the practice of the traditional ICA curve. The voltage and current of the battery are collected by the device, and the capacity is obtained by integrating the time. The voltage interval dV is set, then the dQ/dV is taken as the vertical axis, and the voltage V is plotted on the horizontal axis [5, 6].

Related literatures have dQ/dV as the vertical axis, SOC as the horizontal axis, and use the ICA curve to estimate the battery capacity.

However, the conventional ICA curve drawing method inevitably causes the existence of noise on the curve. As shown in figure 1, the noise has a serious impact on the acquisition of the peak of the ICA curve. The △SOC has a gap of 6.6%. And the existence of noise is independent of the battery voltage acquisition accuracy, the current acquisition accuracy, the size of the voltage interval dV, and whether the value of dV is fixed (and whether the voltage acquisition accuracy is the same order of magnitude as that of dV). Therefore, it is necessary to perform certain filtering and noise reduction processing on the ICA curve to better restore the characteristics of the curve and derive the relevant characteristics of the battery.

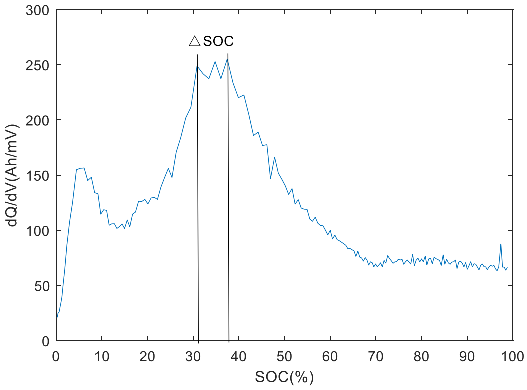

Figure 1. Error at the peak of the original ICA curve

2. Battery experiment design

In this paper, two batteries of the same batch of the same manufacturer are charged and discharged at 25 °C, and the charge and discharge data of the adjacent cycles in 100-200 cycles are taken (it is considered that there is no significant change of the characteristics of the battery during the adjacent cycles). Then Gaussian process regression, wavelet transform are used to denoise the ICA curve to verify whether these methods can better restore the characteristics of the ICA curve.

The battery used in this paper is a domestic manufacturer with a rated capacity of 114Ah ternary battery, the positive electrode material is nickel-cobalt-manganese, and the two batteries are named as battery 1# and battery 2#.

2.1. Battery Test Platform

In this paper, the battery test system of BT2000 model of American Arbin Instrument Company and the constant temperature and humidity test chamber of BTT-544C of Dongguan Bell Test Equipment Co., Ltd. are used to build the battery test platform, as shown in figure 2.

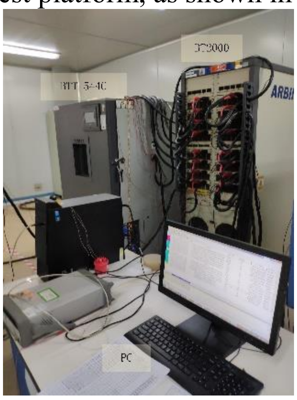

Figure 2. Battery test platform

2.2. Battery test process

The experimental process designed in this paper is as follows:

(1) Allow the battery to stand still in the incubator, where the incubator environment setting: 25 ° C

(2) 90A charge the battery to 4.14V, reduce the current to 38A to 4.25V, and then reduce the current to 5.7A to 4.25V. Allow to stand for 10 min.

(3) 90A discharge the battery to 2.8V with constant current, then reduce the current to 38A and continue to discharge to 2.8V. Allow to stand for 10 min.

Cycle (2) (3) steps. Get the data of the loops in which it is adjacent.

3. ICA curve filtering method

IOP Conf. Series: Materials Science and Engineering **486** (2019) 012075 doi:10.1088/1757-899X/486/1/012075

It can be seen from figure 1 that the ICA curve has certain noise and random error, and it needs to be filtered and noise-reduced by a certain method.

3.1. Influence of voltage interval on ICA curve

The selection of the voltage interval dV has a certain influence on the ICA curve. The ICA curve will show different degrees of noise and error due to the difference of dV. As can be seen from figure 3, the smaller the dV, the larger the noise and error, and the increase of the value of dV can reduce the noise on the curve to some extent. However, when dV increases to a certain value, the noise of dV is not significantly reduced. Therefore, the ICA curve drawn in this paper takes dV to 4mV, and then performs corresponding filtering and denoising processing on it.

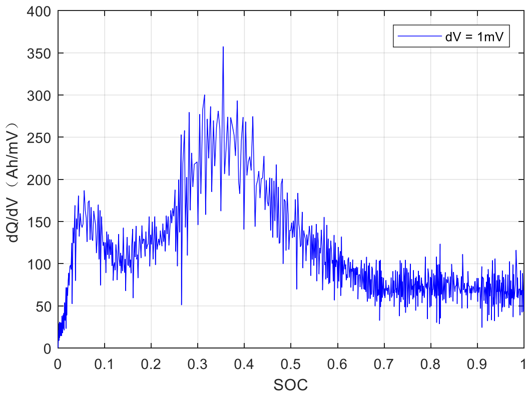

(a) ICA curve with dV = 1mV

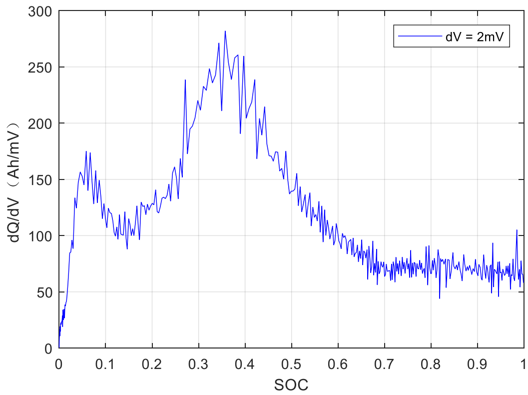

(b) ICA curve with dV = 2mV

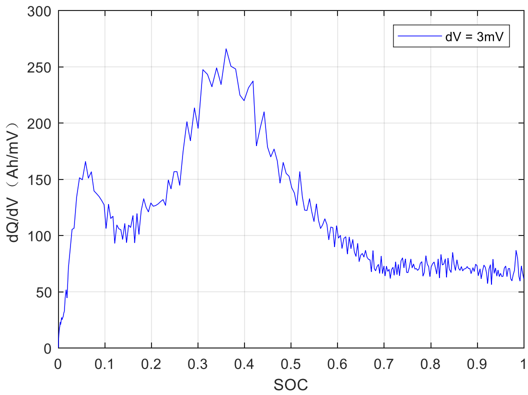

(c) ICA curve with dV = 3mV

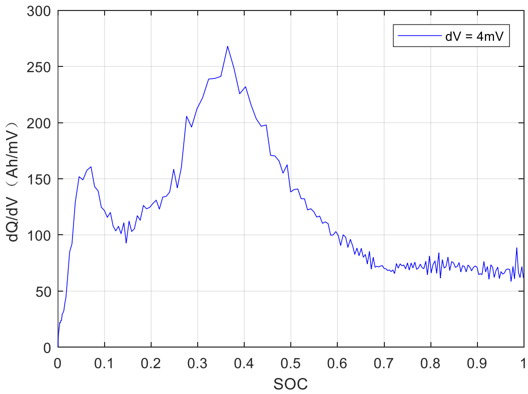

(d) ICA curve with dV = 4mV

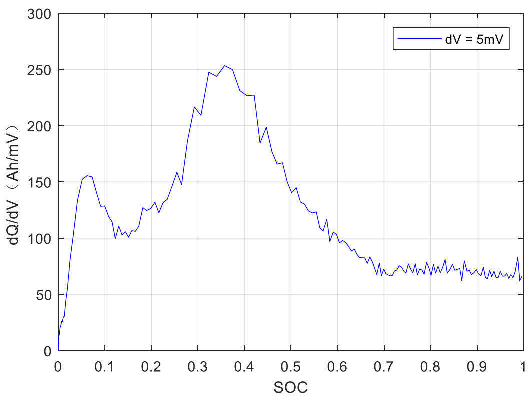

(e) ICA curve with dV = 3mV

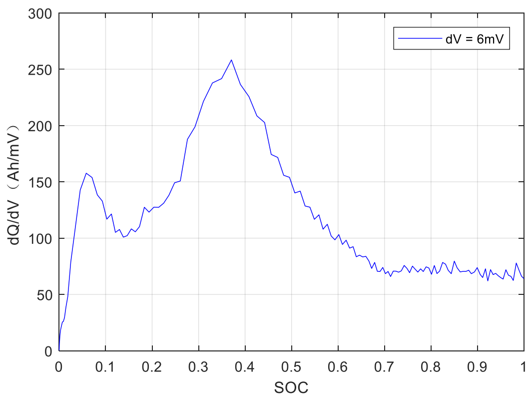

(f) ICA curve with dV = 4mV

Figure 3. ICA curves with different voltage intervals

IOP Conf. Series: Materials Science and Engineering **486** (2019) 012075 doi:10.1088/1757-899X/486/1/012075

3.2. Gaussian Progress Regression

Gaussian Progress Regression (GPR) is a supervised learning process in which the input and output training can be carried out according to the existing observation data (which are subject to the Gaussian distribution) and a predictive model can be obtained to make the output corresponding to the new input as close as possible to its expected value[7].

A key assumption of Gaussian Process Regression is that a certain number of values of X are known, corresponding Y values are modeled, and these Y values are assumed to obey the joint normal distribution.

Gaussian process regression can be seen as two processes: one is the Gaussian process; the other is the regression. The Gaussian process is a Gaussian distribution on a function[8]. The specific form is:

$$f(x) \sim GP(m(x), k(x, x^{'})) \tag{1}$$

In (1):

$$m(x) = E(f(x)) \tag{2}$$

$$k(x, x^{'}) = E((f(x) - m(x))(f(x^{'}) - m(x^{'}))^T) \tag{3}$$

Suppose we observe a training set D:

$$D = \{(x_i, y_i), i = 1, 2, ..., N\} \tag{4}$$

The following model can be used for regression problems:

$$y = f(x) + \varepsilon \tag{5}$$

Where y is the observed value, $f(x)$ is the expected value of the corresponding distribution, and $\varepsilon \sim N(0, \sigma_n^2)$ is the Gaussian noise. It can be obtained that:

$$\begin{pmatrix} \vec{y} \\ \vec{f}_* \end{pmatrix} \sim N\left(\vec{0}, \begin{pmatrix} K_y & K_* \\ K_*^T & K_{**} \end{pmatrix}\right) \tag{6}$$

In (6):

$$K_y = K + \sigma_{\mathrm{n}}^2 I_N \tag{7}$$

$$K = \begin{pmatrix} \mathrm{k}(x_1, x_1) & \dots & k(x_1, x_N) \\ \vdots & \ddots & \vdots \\ k(x_N, x_1) & \cdots & k(x_N, x_N) \end{pmatrix} \tag{8}$$

$$k(x_i, x_j) = \sigma_f^2 e^{-\frac{1}{2\rho^2}(x_i - x_j)^2} \tag{9}$$

$$K_* = \begin{pmatrix} k(x_1, x_*) \\ \vdots \\ k(x_N, x_*) \end{pmatrix} \tag{10}$$

$$K_{**} = k(x_*, x_*) \tag{11}$$

In formula (7), K is the N-th order covariance matrix, also known as the kernel function, and its internal element $k(x_i, x_j)$ represents the correlation between x_i and x_j. From this we can get another important assumption of Gaussian process: the closer the adjacent elements are, the stronger the correlation will be, and all the elements have a certain relationship. σ_{n}^2 is the variance of random noise. I_N is the N-th identity matrix.

Then, the posterior probability distribution of the predicted value f_* corresponding to the new value x_* can be obtained:

IOP Conf. Series: Materials Science and Engineering **486** (2019) 012075 doi:10.1088/1757-899X/486/1/012075

$$f_*|X, y, x_* \sim N(\mu_*, \Sigma_*) \tag{12}$$

In (12):

$$\mu_* = K_*^T K^{-1} y \tag{13}$$

$$\Sigma_* = K_{**} - K_*^T K^{-1} K_* \tag{14}$$

μ_* is the expectation of the predicted value f_*, and Σ_* is the variance of f_*.

Figure 4 shows the filtering and noise reduction of an ICA curve using Gaussian Process Regression. It can be seen from the figure that the original ICA curve with noise can be filtered by GPR, and a smoother curve can be obtained. To a certain extent, the curve can be restored and the real value without noise can be obtained.

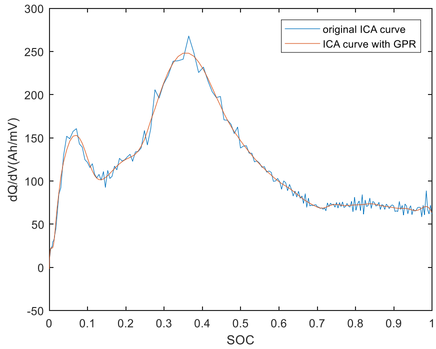

Figure 4. ICA curve after Gaussian process regression filtering

3.3. Wavelet analysis

The concept of Wavelet analysis was first proposed by French Morlet in the 1970s. After that, Meyer and Mallat unified the Wavelet base method and added multi-scale analysis, Wavelet analysis began to flourish. The inherent defect of Fourier analysis in processing non-stationary signals that it cannot obtain the time when frequency components appear has led to the emergence and development of wavelet analysis[9].

The basic idea of wavelet transform is to decompose the signal to be processed into components of different frequency bands and different time periods for further analysis and processing. This process is realized by convolution of the signal to be processed with the wavelet basis function[10]. The definition of wavelet transform is as follows: the wavelet transform of A signal $f(t)$ with finite energy is to translate the parent wavelet function $\psi(t)$ to b, and then take the inner product with the signal to be processed under different scale factors a:

$$WT_f(a,b) = \frac{1}{\sqrt{a}} \int_{-\infty}^{+\infty} f(t)\psi^*(\frac{t-b}{a})dt, a > 0 \tag{15}$$

The size of scale factor a is related to the observation of the whole or part of the signal. When a is large, the resolution frequency is low and the window is wide, which is suitable for obtaining the whole signal. On the contrary, when a is small, the resolution frequency is high and the window is narrow, which is suitable for obtaining the part signal. The positive and negative of the time shift factor b is related to the magnitude of the shift direction and distance.

The one-dimensional continuous wavelet transform has the characteristics of information redundancy. Although it avoids information loss and retains the original characteristics of the information, the large computational amount it brings is what we do not want. Therefore, the discretization operation of the scale factor a and the time shift factor b of the continuous wavelet function can be realized to realize the discrete wavelet transform.

The continuous wavelet basis function can be written as:

$$\psi_{a,b}(t) = \frac{1}{\sqrt{a}}\psi(\frac{t-b}{a}) \tag{16}$$

The general discrete method is to discretize the scale factor a by power series, for example, $a = a_0^j (j \in Z, a_0 > 1)$, if $j = 0$, b are uniformly sampled at a certain basic interval b_0. When $j \neq 0$, sampling along the time axis at intervals of $a_0^j b_0$ still ensures that information is not lost. The continuous wavelet basis function can obtain the discrete wavelet function by discretizing a, b:

$$\psi_{j,k}(t) = \frac{1}{\sqrt{a_0^j}}\psi(\frac{t-ka_0^j b_0}{a_0^j}) \tag{17}$$

Simplified:

$$\psi_{j,k}(t) = a_0^{-j/2}\psi(a_0^{-j}t - kb_0) \tag{18}$$

Among them, a_0^{-j} is called the magnification, and b_0 is the sampling interval. Then get the discrete wavelet transform:

$$WT_f(j,k) = a_0^{-j/2}\int_{-\infty}^{+\infty} f(t)\psi(a_0^{-j}t - kb_0)dt \tag{19}$$

Wavelet transform can be seen as the observation of the signal through the camera lens. The change of the scale factor a can be seen as the expansion and contraction of the lens, so as to observe the part of the signal or the whole picture. The quality factor Q is not changed by the change of the scale factor a. This step-by-step analysis from coarse to fine, from whole to partial, is called multi-scale analysis, and the process is shown in the figure 5. The original signal X is decomposed into two parts, one part is a low frequency signal, that is, a "smooth component"; the other part is a high frequency signal, that is, a "detail portion". The same is true for each subsequent stage decomposition, and the output bandwidth of each stage is halved, so that the sampling frequency can be reduced to half without losing data.

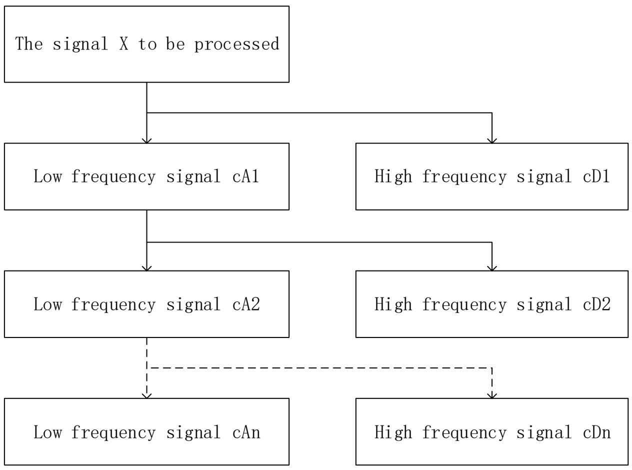

Figure 5. Multiscale decomposition process

Considering the fact that the ICA curve has few values in the middle, the values at both ends are large and the noise is random, the fourth-order Daubechies wavelet function is used to perform the 3-level decomposition of the original ICA data in figure 4, and the low-frequency signal cA3 is obtained as shown in figure 6.

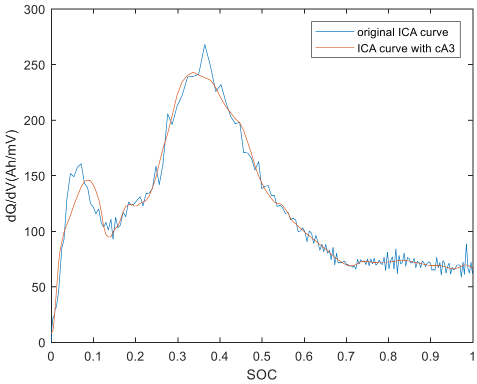

Figure 6. Low frequency signal cA3

Compared with the original signal, cA3 is slightly distorted, and cA2 is obtained by adding the high-frequency signal cD3, as shown in figure 7.

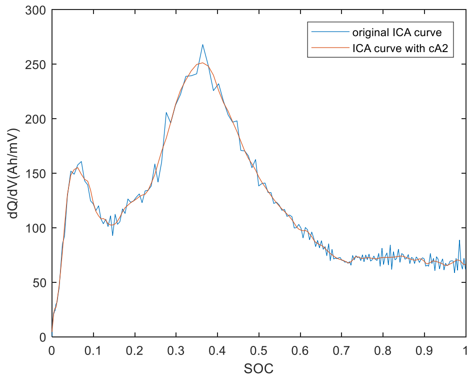

Figure 7. Low frequency signal cA2

The original ICA data, GPR filtering curve, cA2 and cA3 are shown in figure 8. It can be seen from figure 8 that the curve after cA2 and GPR filtering is close to each other.

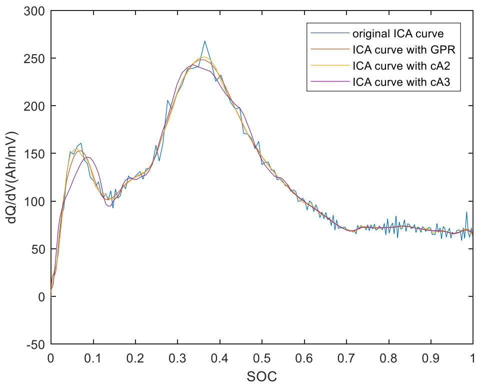

Figure 8. Comparison of several filtering methods

3.4. Experimental results and analysis

ICA curve was made for constant current charging stage by taking charging data of battery 1# adjacent 5 cycles. Since dV=4mV, all data points cannot be guaranteed to be used for ICA curve, and the smaller the dV value is, the more accurate the characterization of the peak is. Four ICA curves were made for 1mV dislocation, and the corresponding capacity values at the peak of four ICA curves were averaged to reduce the capacity error at the peak.

Get the value of capacity at the peak of the original data of ICA curve, ICA curve after GPR filtering, level 2 of wavelet transform, level 3 of wavelet transform and the proportion of the filling capacity and the total charging capacity after the peak are given in σ. See the following tables 1 and 2, Q_p represents the capacity corresponding to the peak, suffix represents the filtering method, and no suffix represents the original unfiltered data.

Table 1 Capacity value at the peak of ICA curve of the battery 1#

Cycles	Q_p	Q_p_gpr	Q_p_ca2	Q_p_ca3
1	29.502092	31.717743	31.723891	33.917775
2	30.805834	31.736293	32.358649	33.596971
3	31.492979	31.804391	32.417791	33.62584
4	30.641931	31.616698	31.616698	33.478269
5	28.03671	31.855129	31.549939	32.801499

Table 2 The ratio of the capacity of the battery 1#ICA curve peak to the total capacity

Cycles	σ	σ_gpr	σ_ca2	σ_ca3
1	0.74355	0.72429	0.724236	0.705166
2	0.732266	0.72418	0.718771	0.708009
3	0.726273	0.723566	0.718235	0.707735
4	0.733639	0.725166	0.725166	0.708984
5	0.756311	0.723122	0.725775	0.714896

Since in the adjacent several cycles, the battery does not change significantly in the external environment without significant change, the σ value will not change greatly, and the mean value of the σ value obtained by different methods is obtained. The variance is shown in table 3 below.

Table 3 Stability of battery 1#σ value

Filtering method	Mean of σ	Variance of σ
no	0.738408	0.000111
GPR	0.724065	4.83E-07
ca2	0.722437	1.06E-05
ca3	0.708958	1.04E-05

It can be seen from table 3 that the value of σ has a large variance, while σ_gp, σ_ca2, and σ_ca3 are relatively stable, wherein σ_gp has the best stability, and σ_ca2 and σ_ca3 have almost the same stability.

Take 9 adjacent cycles of the battery # 2 and do the same operation. Get the capacity at the peak of the battery # 2, σ, the mean value of σ, the variance of σ shown in table 4, table 5 and table 6 below. In table 4 and 5, Q_p still represents the capacity corresponding to the peak, suffix represents the filtering method, and no suffix represents the original unfiltered data.

Table 4 Capacity value at the peak of ICA curve of the battery 2#

Cycles	Q_p	Q_p_gpr	Q_p_ca2	Q_p_ca3
1	28.722211	31.257256	31.583991	33.445772
2	31.196582	31.174024	30.856666	32.775352
3	30.928437	31.182846	30.547828	32.76782
4	28.919037	31.437171	31.129057	32.676549
5	27.321544	31.09956	30.788574	32.989949
6	31.511212	31.511212	30.844604	32.724567
7	30.656161	30.656161	31.272404	32.492698
8	28.931347	31.408842	30.811212	32.361635
9	29.876887	31.140195	31.140195	32.372584

Table 5 The ratio of the capacity of the battery 2#ICA curve peak to the total capacity

Cycles	σ	σ_gpr	σ_ca2	σ_ca3
1	0.748399	0.726192	0.72333	0.707021
2	0.726658	0.726855	0.729636	0.712825
3	0.728979	0.726749	0.732314	0.71286
4	0.746487	0.724413	0.727114	0.713548
5	0.760419	0.72729	0.730017	0.710713
6	0.723666	0.723666	0.729512	0.713026
7	0.731202	0.731202	0.725799	0.715099
8	0.746237	0.724507	0.729749	0.716149
9	0.737914	0.726832	0.726832	0.716022

Table 6 Stability of battery 2#σ value

Filtering method	Mean of σ	Variance of σ
no	0.738885	0.000134
GPR	0.726412	4.38E-06
ca2	0.728256	6.55E-06
ca3	0.713029	7.2E-06

It can be seen from Table 6 that the variance of σ is still large, while σ_gp, σ_ca2, and σ_ca3 are relatively stable. The stability of σ_gp is slightly reduced, and the stability of σ_ca2 and σ_ca3 is almost the same while the stability is slightly. There is improvement, but the stability is still not as good as σ_gp.

Comparing the data of battery 1# and battery 2#, using Gaussian process regression to filter the ICA curve can restore the characteristics of the peak of the ICA curve well, and the effect of wavelet transform is second.

For a certain ICA curve filtering, the GPR and wavelet transform operation time are different, as shown in table 7 below.

Table 7 Comparison of Gaussian Process Regression and Wavelet Transform Running Time

Filtering method	Running Time
GPR	13.08
Wavelet Transform	0.001

4. Conclusions

In this paper, Gaussian process regression and wavelet transform are used to filter ICA curve to obtain smooth ICA curve, which can restore the features of ICA curve at its peak, and the conclusion that Gaussian process regression can restore the features of ICA curve at its peak better than wavelet transform is drawn. However, since Gaussian process regression is a supervised learning algorithm, when the data dimension is large and the data volume is large, the operation efficiency will be reduced. The above filtering methods can be selected according to actual requirements. The two approaches presented in this article have been used in real projects.

Acknowledgments

This work was supported by National Key R&D Program of China (Grant Number 2017YFB1201003).

References

[1] Fei Feng, Rengui Lu, Guoliang Wu, Chunbo Zhu. A measuring method of available capacity of Li-Ion series battery pack[P]. Vehicle Power and Propulsion Conference (VPPC), 2012 IEEE,2012.
[2] Sun Peikun. Research on Estimation Method of Electric Vehicle Power Battery Health Status[D]. Beijing Institute of Technology, 2016.
[3] Ma Zeyu, Jiang Jiuchun, Wang Zhanguo, et al. A research on SOC estimation for LiFePO4 battery with graphite negative electrode based on incremental capacity analysis[J]. Automotive Engineering, 2014, 36(12): 1439-1444.
[4] Liu G , Ouyang M , Lu L , et al. Online estimation of lithium-ion battery remaining discharge capacity through differential voltage analysis[J]. Journal of Power Sources, 2015, 274:971-989.
[5] Xue Nan, Sun Bingxiang, Bai Wei, Han Zhiqiang, Li Na. The mechanism of cyclical decay between composite lithium batteries based on capacity increment analysis[J].Transactions of China Electrotechnical Society,2017,32(13):145-152.
[6] Shi Wei, Jiang Jiu-chun, Zhang Yan-ru, et al. Analysis Method of Capacity Decay Trajectory of Lithium Iron Phosphate Battery[J]. Power System Technology, 2015, 39(4): 899-903.
[7] Liu Yiru, Chen Longzhou, Lin Xingyuan.Application of Gaussian Process Regression in Aeronautical Transient Electromagnetic Denoising[J].Journal of Engineering Geophysics,2018,15(06):771-779.
[8] He Zhikun, Liu Guangbin, Zhao Jingjing, Wang Mingxi. A Review of Gaussian Process Regression Methods[J].Control and Decision,2013,28(08):1121-1129+1137.
[9] Li Yuan.Wavelet Transform and Its Engineering Application [M]. Beijing: Beijing University of Posts and Telecommunications Press, 2010.9~32
[10] Liu Mingcai. Wavelet Analysis and Application [M]. Beijing: Tsinghua University Press, 2008.22~47